Indications for non-terrestrial influences on radon signals from a multi-year enhanced confined experiment

Gideon Steinitz[1], Peter Sturrock[1], Ephraim Fischbach[1], and Oksana Piatibratova[1]

[1]Affiliation not available

November 22, 2022

Abstract

A 10-year data set of alpha and gamma radiation from radon in air has been collected using an Enhanced Confined Mode experiment (ECM; EXP #1). Analysis of periodic phenomena from annual to sub-daily scales of the variation of nuclear radiation from radon reveals: a) Possible multi-year variations; b) Periodic signals which occur in the annual, solar rotation (around 30 days), and daily frequency bands; c) Semi-annual and ternary-annual variations which occur as multiples of the primary annual periodicity; d) Daily variation of 24-hour periodicity which is accompanied by multiples of 12- and 8-hours; e) Non-linear couplings among the annual, solar rotation and daily periodicities; f) Evidence of directionality in the gamma radiation. The setting of EXP #1 is at an above surface outdoor location which is thus subject to large environmental influences. However, the most significant statistical features cannot be attributed to local environmental influences, although there is some similarity in the time domain. The patterns of fundamental geophysical periodicities on annual to daily scales and their modulation by Earth's rotation around its axis, support the suggestion of an non-terrestrial influence, essentially of solar origin. Further investigations of radon decays in the geo-sphere will allow formulation of new geophysical implications.

1

Indications for non-terrestrial influences on radon signals from a multi-year enhanced confined experiment

G. Steinitz[1], P. Sturrock[2], E. Fischbach[3], O. Piatibratova[1]

1) Geological Survey of Israel, Jerusalem, 95501, Israel
2) Kavli Institute for Particle Astrophysics and Cosmology and Center for Space Science and Astrophysics, Stanford University, Stanford, CA 94305-4060, USA
3) Department of Physics and Astronomy, Purdue University, West Lafayette, IN 47907, USA

Abstract

A 10-year data set of alpha and gamma radiation from radon in air has been collected using an Enhanced Confined Mode experiment (ECM; EXP #1). Analysis of periodic phenomena from annual to sub-daily scales of the variation of nuclear radiation from radon reveals: a) Possible multi-year variations; b) Periodic signals which occur in the annual, solar rotation (around 30 days), and daily frequency bands; c) Semi-annual and ternary-annual variations which occur as multiples of the primary annual periodicity; d) Daily variation of 24-hour periodicity which is accompanied by multiples of 12- and 8-hours; e) Non-linear couplings among the annual, solar rotation and daily periodicities; f) Evidence of directionality in the gamma radiation. The setting of EXP #1 is at an above surface outdoor location which is thus subject to large environmental influences. However, the most significant statistical features cannot be attributed to local environmental influences, although there is some similarity in the time domain. The patterns of fundamental geophysical periodicities on annual to daily scales and their modulation by Earth's rotation around its axis, support the suggestion of an non-terrestrial influence, essentially of solar origin. Further investigations of radon decays in the geo-sphere will allow formulation of new geophysical implications.

Introduction

The occurrence of radon in the geological environment has been investigated since the middle of the 20th century [Groves-Kirby et al., 2006; Hartman and Levy, 2005; Toutain et al., 1999; Monin and Seidel, 1992; Ball et al., 1991]. Recently Barbosa et al (2015, and contributions therein) presented an extensive overview of radon research in different scenarios – indoor, tectonic, volcanic, and as a geochemical tracer. Its behavior in the geogas (i.e., air in the subsurface porosity) is characterized by relatively large temporal variations that are significantly different from variations of: a) other trace elements in geogas (other noble gases), and b) variation patterns of other dynamic geophysical systems (atmospheric, tidal). Broad consensus exists that there is no simple and straightforward understanding of the behavior of radon, and this is in despite of the relative ease of tracking radon with nuclear detectors in these environs. This lacuna in the understanding of the underlying principles hampers the development of applications – such as the prevalent suggestion of studying it as a proxy for mechanical-dynamic processes in the seismogenic and volcanic contexts.

Two modes of investigations have been applied at the Geological Survey of Israel (GSI):
A) Research of radon phenomena in geogas has been performed at a spectrum of geological sites in southern Israel since 1990. Emphasis was to perform the measurements at locations and methodologies combining relatively high radon levels and a reduction of above surface atmospheric influences, primarily temperature. The radon measurement techniques used are described in Zafrir et al. (2011).
B) Laboratory experiments in which radon signals observed in nature were simulated have been performed by the GSI since 2007. These simulation experiments of radon signals are the first of their kind [Steinitz et al., 2011; Steinitz et al., 2013a; Steinitz et al., 2014; Steinitz et al., 2015]. They were performed at above surface locations (lab, outdoor) and also in the subsurface. The experiments were based on the application of the Enhanced Confined Mode – ECM (ESM-A Fig. 1). In such a configuration an elevated level of radon in air is maintained within a tight volume (container) by diffusion of radon from an attached radium containing source (industrial, geological). Using such a setup the expectation is, that following an initial buildup, a stable level of nuclear radiation will be attained reflecting a steady state between diffusion and radioactive decay. In contrast with this expectation, systematic temporal variations of the radiation is observed. Large signals occur, the patterns and systematics of which are similar to those of radon signals occurring in geogas (e.g. Steinitz et al., 2011). Observed features include non-isotropy and directionality in the (gamma) radiation pattern from radon in air [Steinitz et al., 2013a; Steinitz et al., 2015], sub-daily periodic signals (Steinitz et al., 2014), as well as short term signals attributable to human activity (Steinitz et al., 2016). Considering the boundary conditions imposed in the ECM system these phenomena were attributed to external influences, including non-terrestrial ones [op. cit.; c].

A key simulation experiment operated by the GSI is a long-term multi-sensor reference experiment (EXP #1), acquiring continuous data at a resolution <1-hour. Results from the first three years (2007-2009) (Steinitz et al. 2011) and a later investigation of the same data sets (Sturrock et al., 2012) pointed to and identified fundamental phenomena combining and crossing issues in geophysics, nuclear physics and astronomy. It was suggested that periodic variations in radon decays reflected an influence, such as might arise from solar or relic neutrinos, or dark matter. Investigations of longer data sets (10 years; Sturrock et al., 2018) substantiated and extended this view.

The last-mentioned investigations addressed the topic of the time variation of nuclear radiation from radon using an astronomical and astrophysical approach. The key inferences from this work are that: a) variation of nuclear

radiation from radon does not arise from a simple variation in concentration (i.e. the number of decaying atoms observed by the nuclear detector); b) nuclear decay processes in the radon system are at least in part of non-spontaneous origin; c) non-terrestrial agents influence the nuclear decay. A possible interaction arising from neutrinos, cosmic or solar, is suggested; d) the nuclear radiation due to decay is anisotropic the parameters of which are related to primary directions of Earth.

Using a 10-year data set with a short-time resolution the present contribution extends the previous investigations by presenting further results. A geophysical approach is applied to the examination, enabling a further insight into the relevant phenomena.

Methods

A detailed description of the experimental setup (ESM-A Fig. 2) is given in Steinitz et al., (2011). The experiment was placed under an open hut, located in the yard of the GSI. It consisted of a 640-liter square iron tank, whose internal volume was sealed from the environment with gaskets and silicon glue. The upper sub-volume of the tank contained air and the lower part of the tank was filled with ground phosphorite containing uranium and radium (^{226}Ra) which serves as the source of ^{222}Rn in the air of the experiment.

Three radiation detectors were inserted into the tank via the vertical tubes on the top, separated from the external atmosphere by gaskets. A gamma sensor (g-C) was inserted into the tank into the central tube enclosed (immersed in the upper third) within a lead pipe (length 30 cm, O.D. 10.5 cm and 0.5 cm thick). A perforated round lead plate was placed at the bottom on end of the lead pipe. This lead shield serves to reduce the direct gamma radiation emitted from the phosphorite while allowing gas exchange between the measurement cell and the air volume of the tank. This configuration leads to detection by g-C of gamma rays in a preferential downward oriented cone of view (see also below).Two alpha detectors were inserted into the other two vertical tubes, flanking the gamma-C sensor. The eastern detector was placed approximately 47 cm above the phosphorite (a-H) and the western one approximately 5 cm above the phosphorite (a-L). Two additional external gamma detectors were fixed to the hut in a vertical position, on the eastern side (g-E) and western side (g-W).

Radiation emanating from ^{222}Rn and its progeny was measured using alpha and gamma detectors of types extensively utilized for long term monitoring in the geological environment (Zafrir et al., 2011). The two alpha detectors are of model Barasol BT45N based on a 450 mm^2 Si diode. The sensitivities given by the producer (Algade Inc., France) for sensor a-H is 42.6 Bq/m^3 per 1 count/hour and 51.9 Bq/m^3 per 1 count/hour for sensor a-L. Gamma radiation is measured using 2"×2" NaI(Tl) detectors (PM-11, ROTEM Inc., Israel), recording gamma-ray impulses of energy above 40keV. Utilization of gamma detector systems for monitoring radon was based on the detection of gamma radiation from the ^{214}Bi decay, and to a lesser extent those from the ^{214}Pb (Zafrir et al., 2011; see Table 3 therein). ^{214}Bi decays via β$^-$ (99.98%) and via α (0.02%). Due to the short half-lives of the radon daughters, equilibrium of the radon and its daughters is achieved after a short time (~25 minutes) (ESM-A Fig. 3).

Data acquisition at intervals of 15-minutes was with dataloggers (Campbell Inc.) which also supplied the stabilized power to all detectors by a continuously loaded 12V supply battery. Since power was supplied by a battery, rather than line current, fluctuations in line voltage cannot account for any periodicities observed in the data. Ambient temperature and barometric pressure were measured at the datalogger console (DL). In the serial representation of the date, Day 0 is 1.1.1992. Timing is based on UT. The experiment, located on the premises of the GSI in Jerusalem is in time zone UT+2.

Results

The five nuclear detectors of the experiment record different attributes of nuclear radiation (ESM-C). The two alpha detectors are influenced by radon within their sensing cup (scale of few cm). The volume of the sensing cup is in equilibrium with the air of the tank – i.e. with the concentration of radon in the air of the tank. The central gamma sensor is in the vertical position and within a 0.5 cm thick vertical Pb pipe. This position and orientation of the sensor results in preferential absorption of gamma rays in the air below the sensor and from the upper part (~30 cm) of the phosphorite. The lateral sensors gamma-E and gamma-W are affected by horizontally oriented gamma radiation evolving from the air volume of the experiment.

Overview of nuclear radiation at the internal sensors

Using daily averages the temporal variation of the nuclear radiation inside the tank during 8 years (2007-2015; Days 5520-8446) is shown Figure 1.

The count rate at the gamma sensor is on the order of 2.3 E+5 counts (per 15-minutes) and around 1300 counts at the alpha sensors. In these plots the annual variation dominates the patterns, and a semi-annual periodicity is also observed. Further variations, of shorter wavelength are superimposed on the annual variation. These are composed of multi-day variations and systematic daily signals (Steinitz et al., 2011).
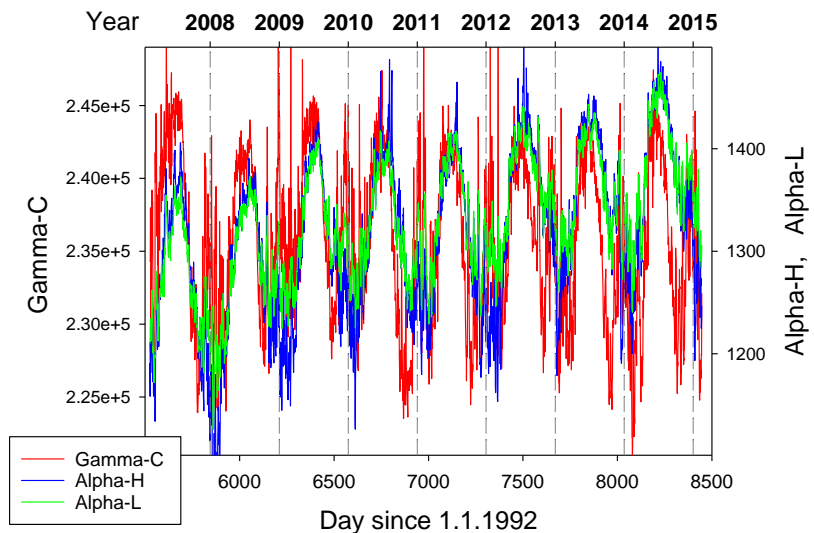

Figure 1: The temporal pattern of gamma and alpha radiation measured by the internal sensors. The plot is based on daily average. 8 years are shown. The vertical dotted lines denote 1st of January.
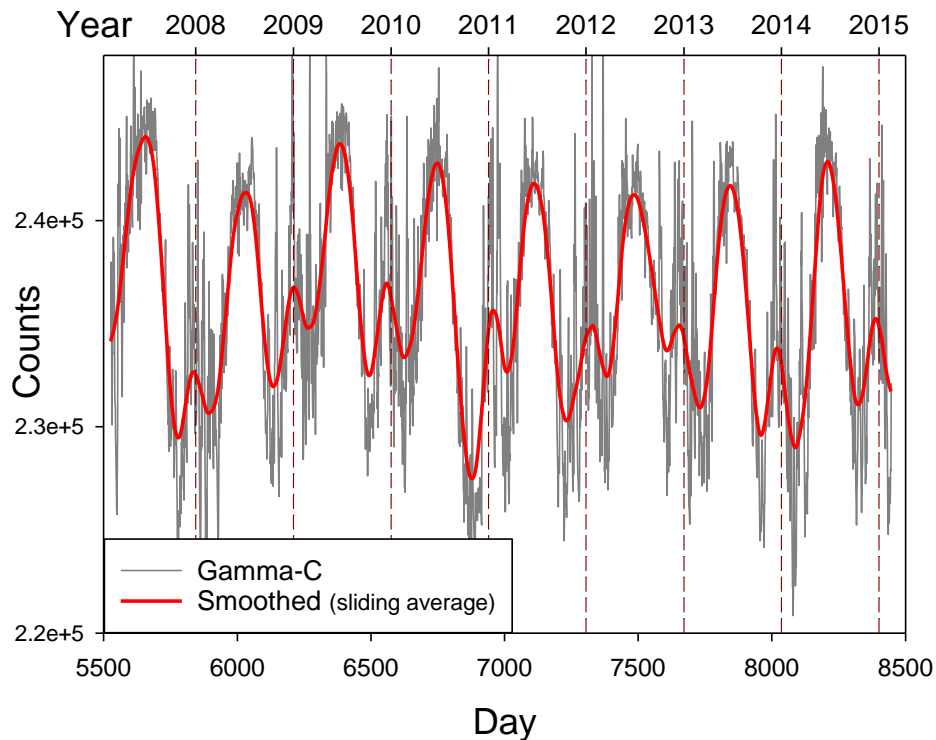
4

Figure 2: Temporal variation of the gamma-C signal, using daily averages, in in the air volume of the tank. Smoothing the time series with a two-stage sliding average shows that annual scale variation is composed of a large annual and a significant semi-annual s

Figure 2 presents the time series of gamma-C (daily averages; shown in Figure 1) and a plot of the smoothed data, demonstrating in the time domain the occurrence of a semiannual variation, in addition to the annual one. These features are accentuated when analyzed in the frequency domain. Spectral analysis (FFT) of 10-year time series of the daily averages demonstrated that annual and semiannual signals occur in gamma and in alpha variation (Figure 3). Furthermore, a ternary annual variation is also indicated (g-C).
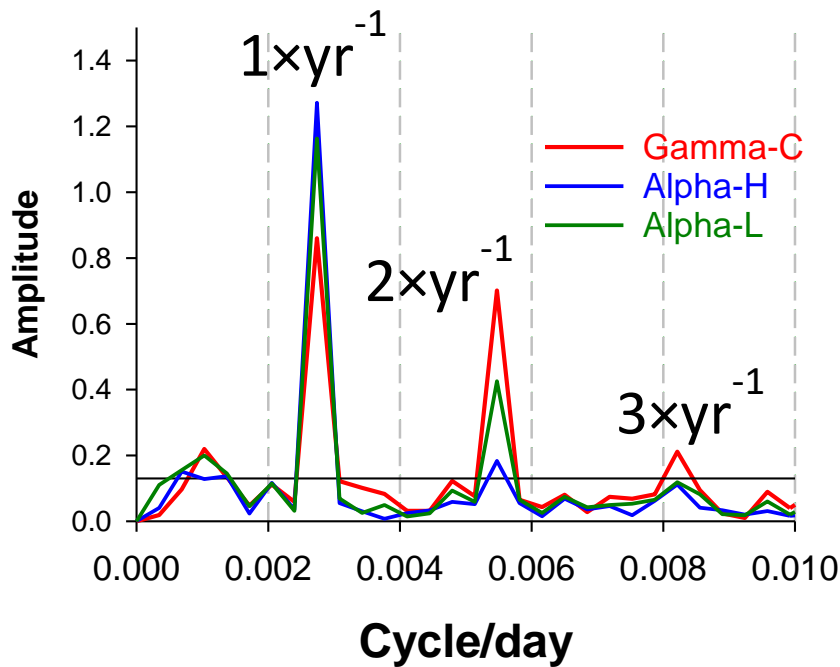
Figure 3: Spectra (FFT) of the time series (daily averages) of the internal gamma and alpha detectors. Annual, semiannual and possibly also ternary annual periodicities are indicated. The confidence level (99.9%; horizontal line) is also shown.

Statistics of variation in the 24-hour window

Data in the experiment are collected at a resolution of 15-minutes. This fact, along with the continuity and completeness of the data sets over a time span of 10 years allows a detailed of statistical analysis of the variation within the 24-hour cycle to be carried out. Each 10-year time series is linearly de-trended and normalized, to allow comparison of values among the sensors. These normalized time series are decomposed into 96 15-minute time series. Each decomposed time series contains one 15-minute measurement per each day in the serial sequence. Statistical descriptors are calculated for each decomposed time series and the results are presented per Hour-in-Day (HID). Thus the first entry in the series comprises all data between 00:00 and 00:15 (UT), and the last are the data between 23:45 and 00:00 (UT).

Figure 4 presents the average variation of the normalized signal at the internal nuclear sensors as a function of HID:

- The lower alpha sensor (a-L) shows a varying signal with maximum around hr-6 and minimum at hr-14, i.e. within 8 hours.

6

- The upper alpha sensor (a-H) shows a stable level in the interval from hr-21 to hr-10. A strong symmetric negative peak occurs in the interval from hr-10 to hr-21m (a difference of approx. 12 hours), with a minimum around hr-16.
- The central gamma sensor (g-C) depicts a low stable level from around hr-21 to hr-5 (a difference of approx. 8 hours). A strong peak is developed in the interval from hr-5 to hr-16, with a maximum around hr-11. A secondary peak with a maximum at hr-17 and with a relative amplitude of 20%, occurs on the decreasing limb of the main peak. A time difference of 6 hours occurs between the maxima of the main peak and the secondary peak.
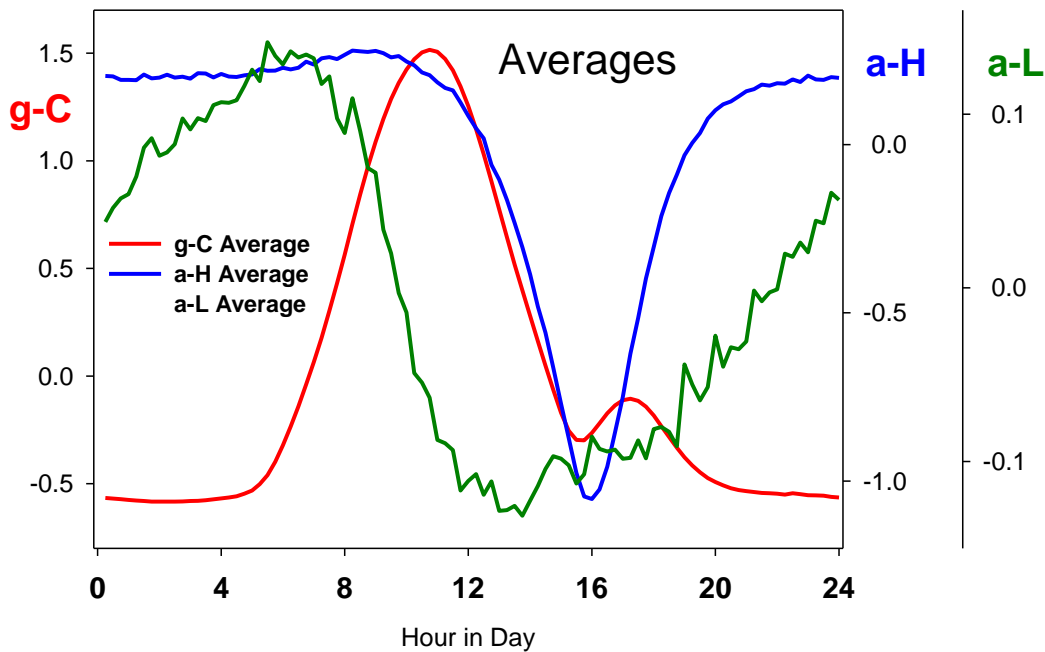
Figure 4: Variation of the average as a function of HID at the internal nuclear detectors. Different relative variation scales occur.

The above daily variations of the averages of the nuclear radiation (Figure 4) are compared in Figure 5 (left) using a mutual normalized scale. In the case of the internal nuclear detectors (left) the largest variation is at g-C. The variation of a-L is subtle relative to a-H albeit the count rates are similar. The daily variations of ambient temperature and barometric pressure are plotted on the right at the same relative scale. Clearly different daily patterns are indicated for the internal alpha and gamma sensors. The sensitivity of the two alpha sensors is similar and both record a similar count rate. Still, the daily variation at the lower alpha sensor (a-L) located close (5 cm) to the source material is much lower and differs from the variation at a-H, situated 47 cm above.
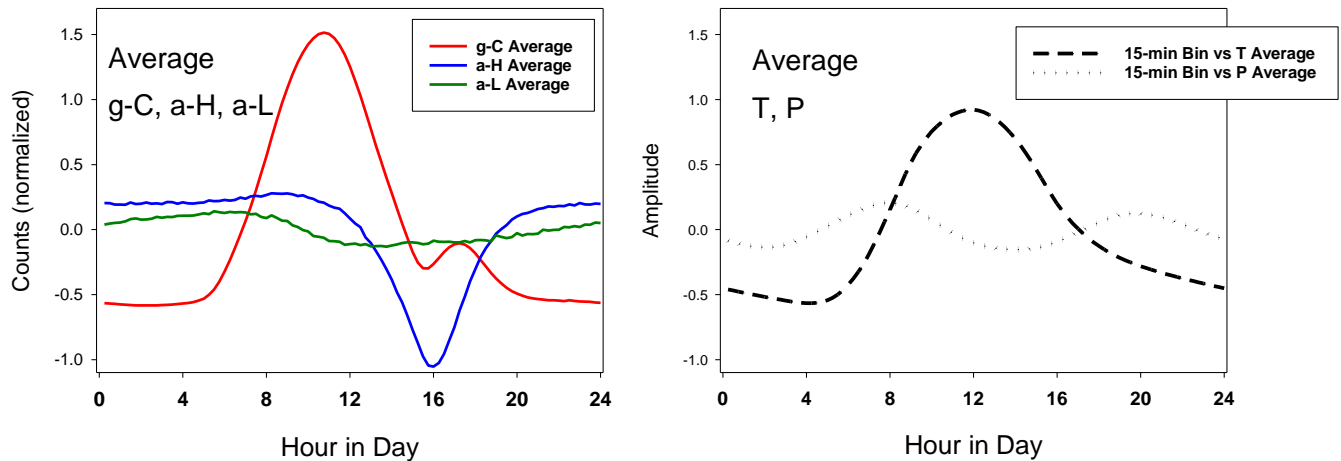
Figure 5: Comparison using the same normalized scale of variation of the daily variation of averages at the nuclear detectors (left), and ambient temperature and barometric pressure (right).

Temperature shows a peak around noon and pressure shows two peaks per day, of similar low amplitude. The secondary peak in the g-C HID pattern has no parallel feature in temperature. The decreasing flank of the g-C mid-day peak may relate to the negative peak of a-H.A similarity among the general HID pattern is observed between g-C and temperature. Taking into account that the presented HID patterns are derived from a 10-year data set it is be noted that: a) the maximum of the normalized count rate of g-C (1.51) is 50% stronger than the maximum of temperature (0.92); b) the maximum of temperature (12:00 UT) lags the maximum of g-C (10:75 UT).
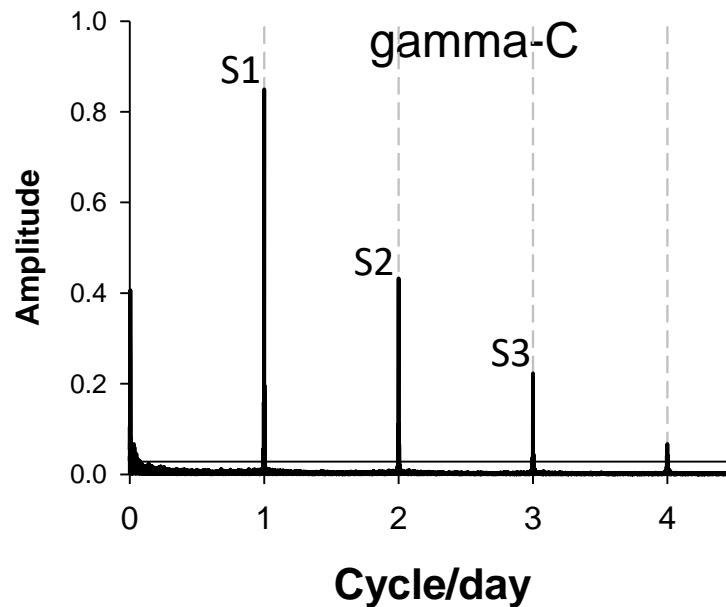
Figure 6: Spectra (FFT) of measurements of g-C. The confidence level (99.9%) is also shown.(A 99.9% critical limit is that level where in only 1 of 1000 separate random noise sets would the largest peak attain this height.)

The spectral pattern in the daily frequency band of the measurements at g-C is shown in Figure 6. The early publication of results from this experiment (Steinitz et al., 2011) already indicated a primary 24-hour periodicity in the time series of the internal sensors (gamma and alpha), as well as multiples of 12-, 8- and even 6-hours. The 24-hour periodicity (S1) is due to a physical influence that is clearly related to rotation of Earth around its axis. The multiples reflecting periodicities of 12-hours (S2) and 8-hours (S3) are large and very significant. In many cases of radon variation analysis the cause of the multiples is either disregarded or they are attributed to reflect harmonics generated in the FFT calculation process, due to features such as non-sinusoidal variation, leakage etc. It was therefore suggested (Steinitz et al., 2011) that the harmonic multiples are also due to the influence of a physical process having geophysical periodicities of S1, S2, and S3. The above integrated time domain (10- years) analysis (Figure 4; Figure 5 and see also Figure 7) constitutes a confirmation (in the time domain) that the above multiples, as observed in the frequency domain, are actually physical phenomena arising from the variation of nuclear radiation from radon.

The setup of EXP #1 consists of three gamma sensors (ESM-A Fig. 1). The central gamma-C sensor is in a vertical position and is enclosed within a 5mm thick Pb pipe. The configuration is such that it is affected primarily by gamma radiation from below. At the two external and lateral gamma detectors variability of gamma radiation (due to radon) is in the horizontal dimension. Figure 7 compares the daily pattern of the gamma radiation at the

9

internal sensor (g-C) and the laterally located sensors (g-W, g-E). The overall variation at the lateral sensors is around 25% of the variation encountered at g-C. The HID patterns of the lateral sensors are similar with a primary negative peak around 13-15 hours (UT). A subsidiary positive peak occurs in g-W around 17 hours.

The clear inverse patterns of the primary HID variation at g-C versus the two lateral sensors is a strong indication for directionality in the time varying gamma radiation from radon in the air of the tank. The association of the directionality with the 24-hour cycle implies an influence linked to the rotation of earth around its axis. The subsidiary peak, around 16-17 hours, which is positive in g-C and g-W suggests a further and separate periodic feature which is superimposed on the daily rotational pattern. The directionality and its patterns suggests the possibility of a non-terrestrial influence. Obviously such directionality cannot be related to environmental influences.
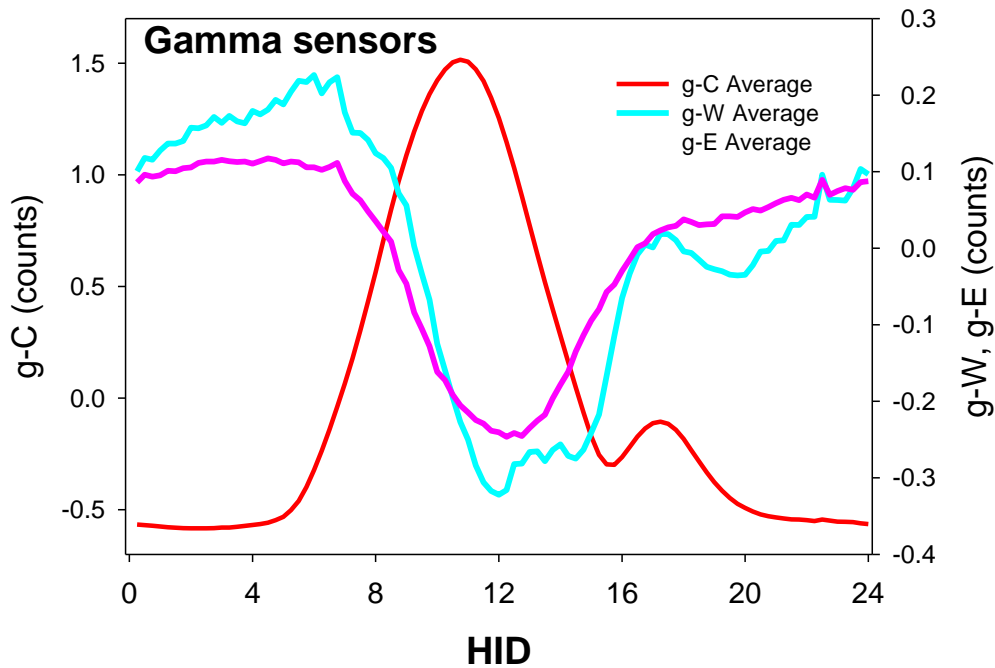
Figure 7: Comparison of the daily variation of averages at the internal gamma detector (g-C) and the lateral gamma detectors (g-W, g-E; Error! Reference source not found.**). Normalized values are used. See text.**

The characteristics of barometric pressure and ambient temperature around and inside the experimental volume was also detailed by Steinitz et al. (2011). Internal air pressure follows the barometric variation. Likewise, temperature variation inside the tank is governed by the ambient temperature. Furthermore, combining detailed analysis of the data subsets, in time- frequency and especially in the frequency-time domains, showed that notwithstanding a general similarity, the daily radon signal is not likely due to local diurnal variation of pressure and temperature. The present evaluation (Figure 4, Figure 5 and Figure 7) of the average variations within the 24-hour cycle of the alpha and gamma radiation (internal; and external sensors) vary in patterns which differ from those of temperature and pressure. This further supports the conclusion that the observed fluctuations in count rate are not entirely due to variations in environmental parameters such as temperature and pressure.

The 24-hour variation of the daily averages is also reflected in patterns of specific hourly time series, as presented in Figure 8. In the shown example two hourly time series of gamma-C separated by 12 hours depict very different but systematic temporal patterns occur over a 10 year time span. The observed integrated time-domain HID pattern of the nuclear radiation from radon in the experiment is used as a basis and starting point for further characterization below of radon phenomena in the frequency domain.
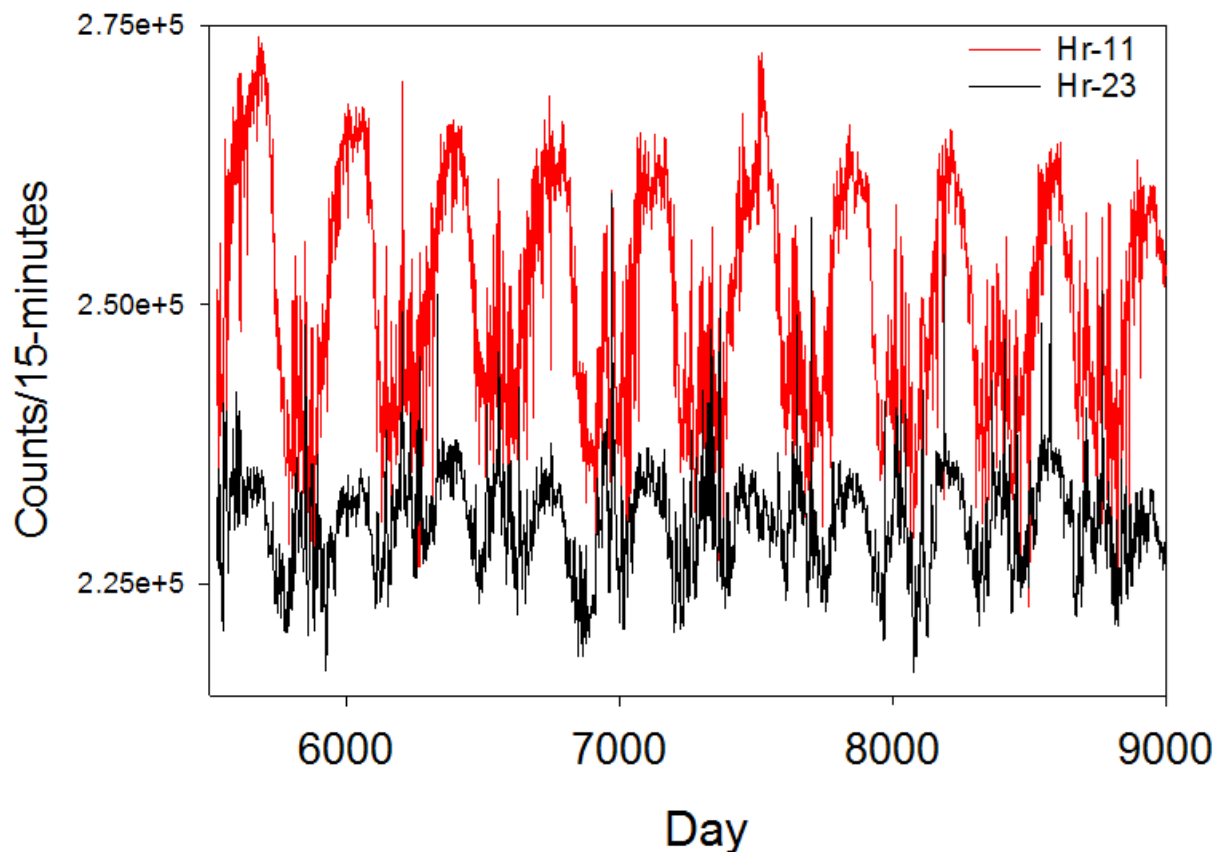
Figure 8: Two hourly time series of gamma-C, 12 hours apart (see also Figure 7).

11

Day-night differentiation of Annual and Solar Rotation oscillation

Recently Sturrock et al. (2018) demonstrated a strong differentiation in the annual frequency band of day-time and night-time measurements. ESM-A Fig. 4 shows that the annual frequency is strong in day-time measurements, and the semiannual in nighttime measurements.

These Solar Rotation (SR) periodicities are interpreted (Sturrock et al., 2018) as reflecting the rotational pattern of internal sectors of the Sun around its axis . In general, the frequency band of SR spans from 6 to 16 year^{-1}.

The occurrence of phenomena attributable to periodicities of Solar Rotation (SR) in an 8-year time series of gamma-C was indicated by Sturrock et al. (2012), and further justified with 10-year data by Sturrock et al. (2018). The two most significant SR periodicities, indicated mainly in night-time measurements, occur at 11.35 and 12.35 year^{-1}.   ESM-A Fig. 5 shows that strong oscillations in the candidate SR frequency band $10 - 14$ year^{-1} (peaks at 11.35 year^{-1} and 12.64 year^{-1}) in the nighttime data, but comparatively small oscillations in the daytime data.

The significance of the daytime vs. nighttime was further investigated by Sturrock et al. (2018; Figs 13-16) using spectrograms displaying the power of oscillations (z) as a function of Hour in Day (x; 24-hour cycle) and frequency (y). The analysis covered data for g-C, as well as ambient temperature, barometric pressure and voltage of supply. The analysis was performed for the annual and solar frequency bands. For the annual band, it was shown that: a) The annual frequency contains a strong power centered around noon whereas temperature, pressure and voltage show a uniform power of the annual frequency over the 24-hour cycle; b) A semiannual periodicity is indicated only in gamma-C, primarily at night. Similar analysis in SR band showed that: a) Oscillations in the gamma-ray measurements occur at or near midnight, but the same is not true for the temperature or pressure measurements; b) The maximum power for the environmental measurements (4.6 to 8.5) are all smaller than the maximum power for the gamma-ray measurements (21.0). These patterns suggest that the annual oscillation and the SR oscillations found in the gamma-ray measurements are not likely attributable to environmental influences.

The interplay among the annual, SR and daily oscillations in the pattern of gamma radiation was further analyzed in the frequency domain using the FFT. High time resolution data of g-C during 10 years was de-trended by applying a double sliding average (61 and 51 days). Applying FFT to the de-trended time series shows that the SR (~31 days = 0.032 cpd) periodicity is observable in the FFT spectrum (Figure 9).
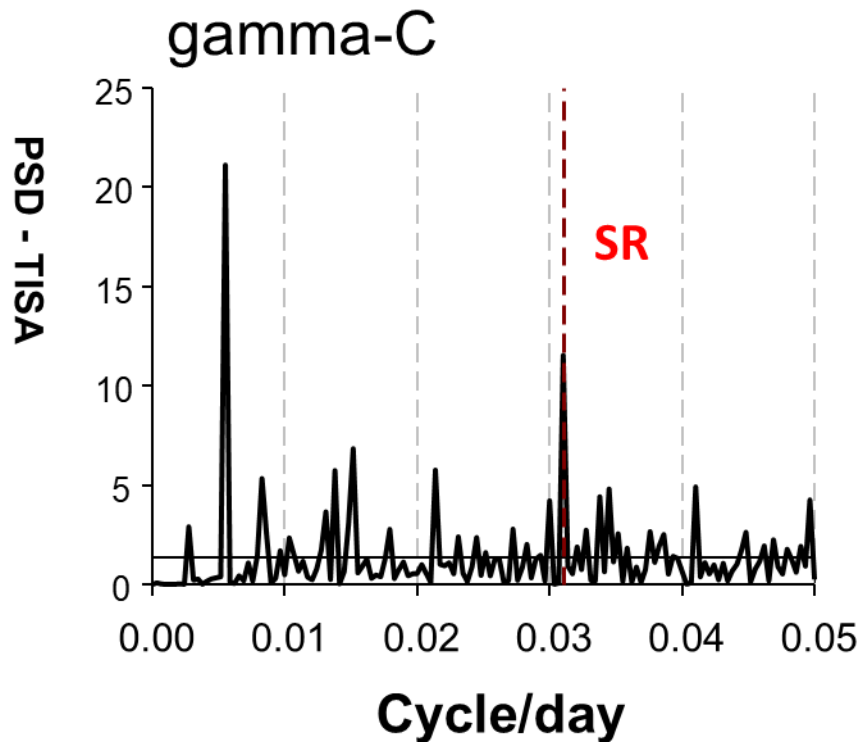
Figure 9: Spectra (FFT) of 10-years of 15-minute measurements at gamma-C. The data were de-trended to remove the large annual variation. The band denoted by SR corresponds to a periodicity of ~12.3 yr-1 = ~0.034 cycle/day, the synodic rotation period of the Sun.

Linearly de-trended (and normalized) 15-minute time series of g-C was decomposed per 15-minute bin of the daily cycle – yielding 96 (independent) time series each containing one specific 15-minute measurement bin per day. The amplitude of the annual and SR frequencies was extracted by FFT for each bin-specific time series. Plotting (Figure 10) the variation of the amplitudes of the annual and SR frequencies as a function of HID reveals continuous variation pattern as a function of HID. The patterns conform with the plots, given in Figures 13-16 of Sturrock et al. (2018) which were derived from hour averages using a different analysis mode. Using a 15-minute resolution smooth variation patterns are encountered over the 24-hour daily cycle. The amplitude of the annual periodicity is strong in measurements obtained from Hr-8 to Hr-13 (UT), with a secondary peak (20%) around Hr-17. The main variation of the SR periodicity shows a pattern inverse to the annual one having a significant minimum in the interval of Hr-8 to Hr-14. A secondary (20%) peak occurs around Hr-16. The analysis for g-C, in both modes, shows that rotation of earth around its axis (24-hours) jointly modulates the annual and SR periodicities. As SR is independent of the rotational relations of the Earth-Sun system this forms an independent indication of an non-terrestrial influence.
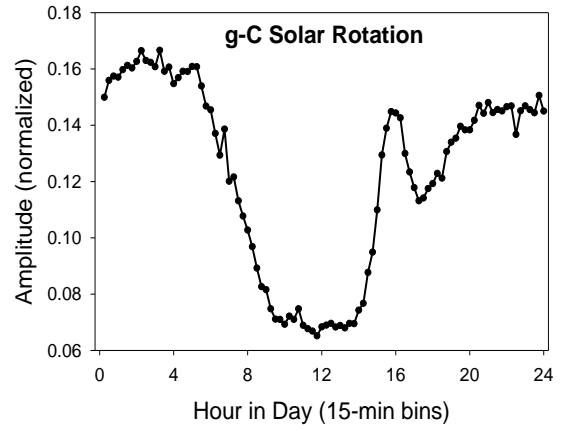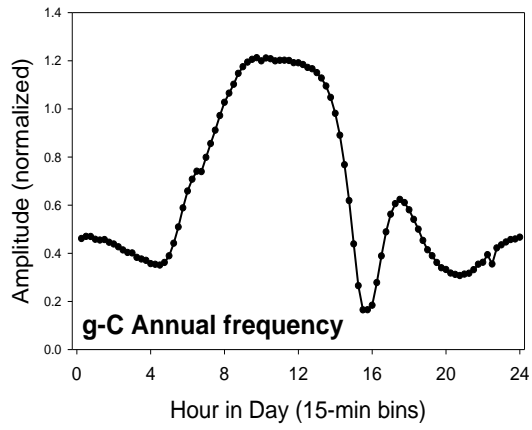
Figure 10: Amplitudes (FFT) of Annual (left) and SR (right) frequencies as a function of the Hour-In-Day (HID). See text.

The variation of the amplitude of the semiannual and ternary annual oscillations as function of HID was also determined, in an analogous way. A comparison of the HID patterns of the primary and multiples in the annual band is shown in Figure 11. Systematic variation over the 24-hour cycle occurs also in the multiples of the annual frequency. The semi-annual (yr^{-2}) pattern shows an inverse pattern compared to the annual (yr^{-1}) one. A more complex, but still related pattern is exhibited by the weaker ternary-annual (yr^{-3}) periodicity. All three patterns show a subsidiary feature around 16 hours.

In the case of g-C the quality (strength) of the annual signal allowed us to also determine the phase and the specific frequency of the annual periodicity in each 15-minute bin (using the same FFT analysis). Figure 12Figure 12 shows for the annual periodicity the variation of phase and frequency as a function of HID, along with the amplitude. Smooth patterns occur. A strong relation among the three parameters is evident – for the primary daily (24-hour) pattern as well as the secondary variation around 16-hours. These three FFT characteristics of the annual periodicity – amplitude, phase and frequency – are independent parameters. The immediate conclusion is that the gamma radiation from radon and its daughters, due to nuclear decay, displays a unique nonlinear interaction arising from the annual and diurnal periodicities. Such patterns and relations cannot likely be attributed to "environmental" influences. On the other hand, the strong relation between cyclic phenomena of diurnal and annual scale imply, again, that an non-terrestrial driver influences the nuclear decay of radon (Bi-214). These detailed characteristics of nuclear radiation in the frequency domain, which are related to the timing of the measurement in the 24-hour cycle, point to phenomena yet to be understood.
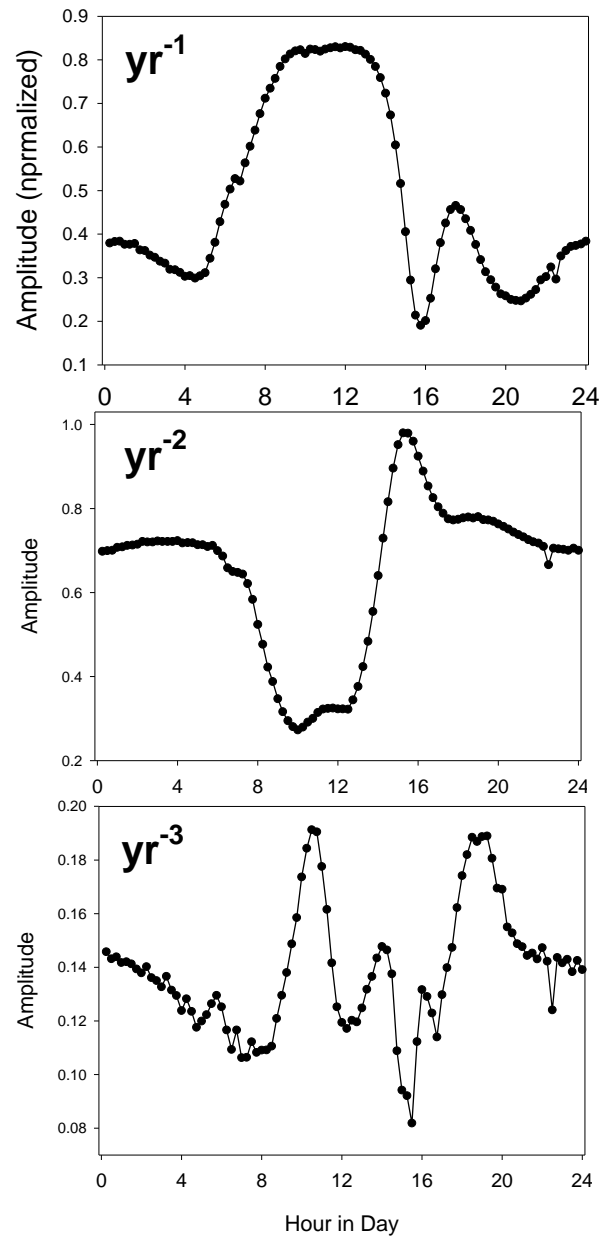
Figure 11: Comparison of the amplitudes of periodicities in the annual frequency band. See text.
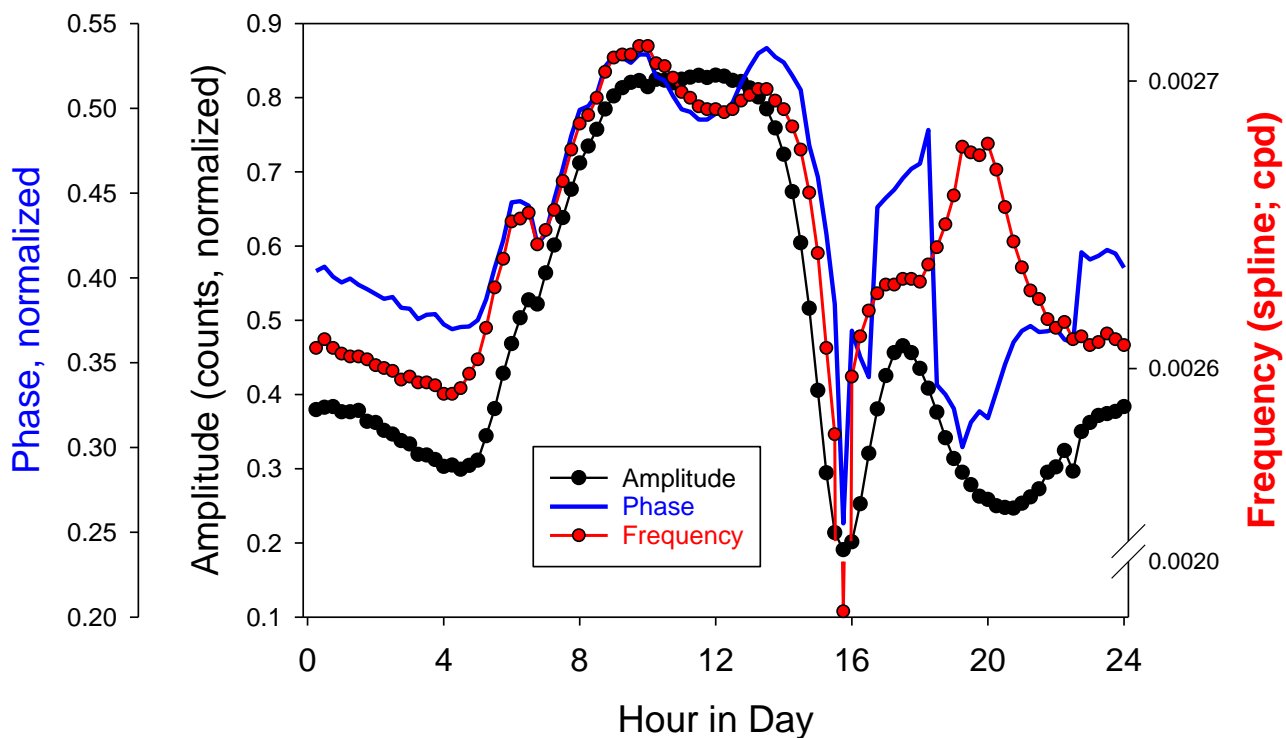
Figure 12: Relation of phase and frequency of the annual periodicity at gamma-C as a function of HID. The pattern of the outcome is based on data spanning 10 years at a resolution of 15-minutes. The precise frequency is determined from a spline fitted to the amplitude of the annual peak. See text for further discussion.

Comparison of annual and daily variation at the internal and external gamma sensors

The setup of EXP #1 (ECM-A Fig. 2) comprises two lateral gamma sensors in addition to the internal g-C. These lateral sensors (g-W; g-E) are placed at opposite sides of the tank, at the level of its upper air volume. The sensors, in a vertical orientation are protected inside PVC tubes. Signals due to gamma radiation from the tank are recorded. Blocking g-E to the gamma radiation from the upper volume of air in the tank (only, not to the phosphorite in the lower part) halved the count rate from a level of around 1.8×10^5 to around 7.5×10^4 (Counts/15-minute; Steinitz and Piatibratova, 2008). Thus the "field of view" of the lateral sensors is comprised of gamma radiation from the air volume of the tank, radiating in opposite directions within the horizontal dimension. The field of view of the internal g-C is primarily downward looking.

Using daily averages Figure 13 shows the long-term variation at the lateral sensors, installed outside the tank at opposite directions (g-West, g-East). A clear annual modulation with a maximum in winter is evident at both sensors. In contrast the internal gamma sensor (g-C; and also a-High, a-Low; see also Steinitz et al., 2011) show an annual modulation with a maximum in summer (Figure 1). This geometrical difference in the timing of the annual maximum indicates a directionality in the radiation pattern.
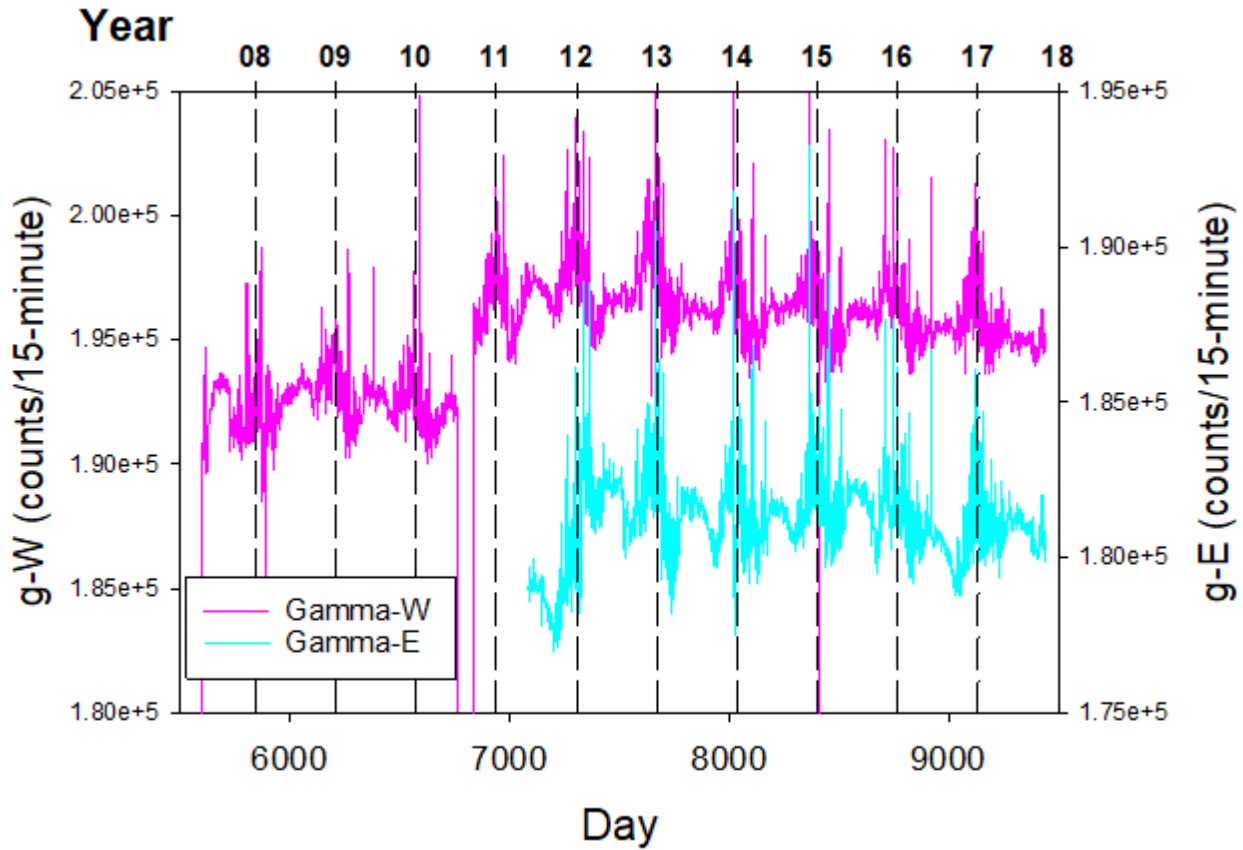
Figure 13: Multi-year pattern of variation at the lateral gamma sensors (g-W, g-E). Daily averages are used. The annual peak occurs in winter. See text.

A similar directional difference is observed in the case of the daily variation as shown in Figure 14. The patterns indicate a mid-day maximum if the case of g-C and mid-day minima in the case of the opposite lateral sensors. These corresponding different patterns of the annual and daily signals reflect directionality in the time variation of radon signals. Again, it should be noted that local environmental variation cannot naturally account for such directional relations.
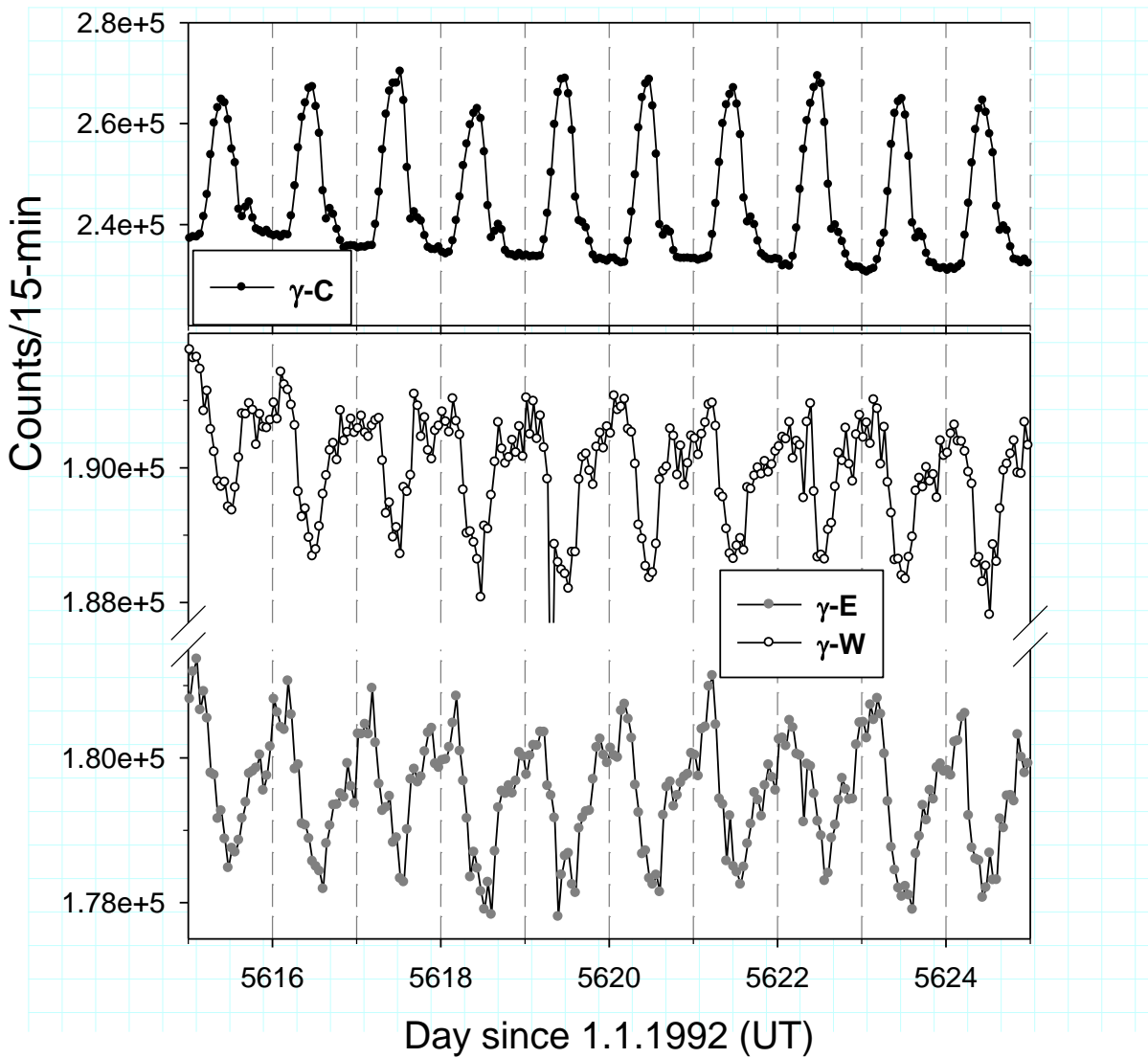
Figure 14: Comparison during a 10-day interval of the daily variation at g-C and the lateral gamma sensors. See text.

Summer peak time (SPT)

The variation of the gamma and alpha radiation at the internal sensor of EXP #1 exhibit a large annual signal (Figure 1; Figure 2), with a peak in summer. Ambient temperature is a typical environmental parameter with an annual maximum in summer. Using 3.5 years of data Steinitz et al. (2011; Figure 9 therein) indicated a time shift among the summer maxima of the gamma, alpha and temperature patterns. The SPT of gamma radiation (g-C) preceded the similar SPT of the two alpha detectors and the SPT of temperature.

Using the 10-year data set the SPT as measured by the internal sensors (g-C, a-H, a-L) and temperature was determined. Time series of daily averages were linearly detrended and normalized. Using the Continuous Wavelet Transform (CWT) the annual variation was reconstructed in the range of 0.0026-0.0028 cpd (= around yr^{-1}; see Figure 9). The resulting filtered time series (Figure 15) display similar curves having systematic offsets among them. From these reconstructed time series the annual maxima are extracted to determine the Day-in-Year (DIY) of the SPT.
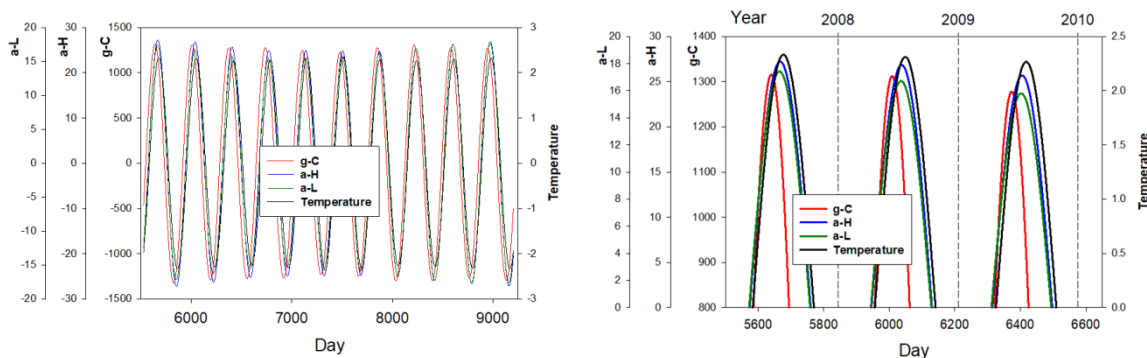
Figure 15: The filtered annual signal at the internal nuclear sensors and ambient temperature based on daily averages. The reconstruction is by CWT filtering in the range of 0.0026-0.0028 CPD. Left – the 10-year pattern; Right – three year detail demonstrating di

Figure 16 shows, for the years 2007 to 2016 the dependence of SPT on the Day-In-Year (DIY). Systematically different and smooth SPT curves are obtained. SPT of temperature lags SPT of g-C by 30-40 days. Such a lag is in the order 8-10 half-lives of Rn-220. Adjacent SPT patterns are obtained for the two alpha detectors – occurring between those of gamma-C and temperature. A systematic multi-year variation is indicated for the nuclear radiation.

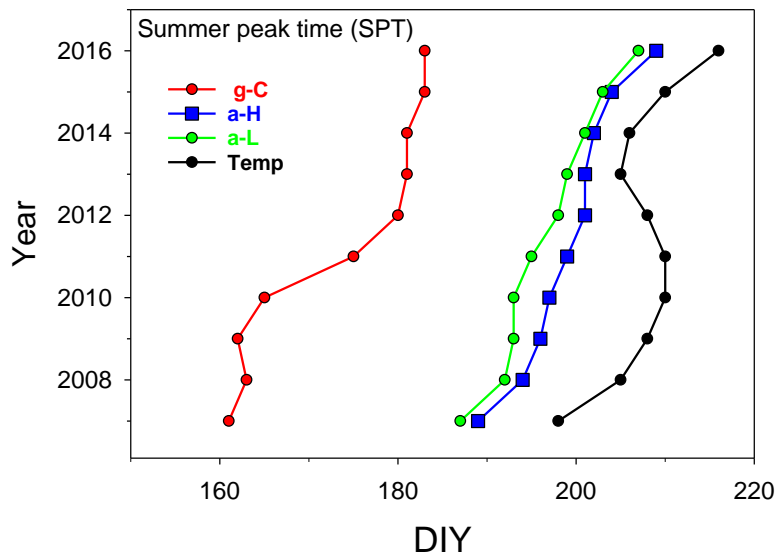| Day-in-Year (DIY) of Summer-Peak-Time (SPT)		
Sensor	Mean (DIY)	StDev (days)
g-C	173	9
a-H	199	6
a-L	197	6
Temperature	208	5

Figure 16: The distribution of DIY of SPT in the years 2007-2016, for the three internal nuclear detectors and ambient temperature. The analysis is based on daily averages. See text for further details.

The results of the examination of the SPT of the annual variation during 10-years are summarized as follows:

1. Different SPT patterns are observed for the gamma and alpha radiation from radon in the experiment. Both differ from the SPT pattern of temperature.
2. The multi-year variations suggest an non-terrestrial cause for the annual signal in the time series of the nuclear detectors.
3. Separate variants of the external and remote driver are indicated as stimulators of gamma and alpha decay.

4. The patterns for the nuclear radiation are not obviously related to temperature. The often mentioned apparent similarity of annual patterns among temperature and radon does not necessarily imply causality.
5. Multi-year variations are indicated.

Discussion

EXP #1 was set up as an experiment simulating nuclear radiation from radon in air within a confined enclosure. The distinctiveness of the experimental setup related to the following:
1. It is located at an above surface situation, in the lowermost atmosphere
2. It addresses alpha and gamma radiation from radon
3. Applies a multi-sensor configuration
4. Produces 10-year time series collected at a time resolution of 15-minutes.
As such it is a first geophysical reference setup of its kind.

The eventual influence of local environmental conditions is discussed in ESM-B.
The data of EXP #1 are obtained in an outdoor setup configured and installed to test the possibility of simulating radon signals that occur in geological environs. This setup leads to its being influenced by above surface climatic conditions, including a temperature regime spanning 40°C. The confined conditions inside the experiment are assumed to be a good first order simulation of conditions at subsurface locations, especially those where significant transfer and transport of geogas are not expected – which is the majority of cases.

It should be stressed that this contribution and the work of Strurrock et al., (2018) represent independent analysis of data from the same experiment. The most important result obtained by Sturrock et al. (2012) and Sturrock et al. (2018) on the radon data from the g-C sensor of this experiment is the identification of periodicities in the frequency range 10-16 yr^{-1} associated with solar rotation (SR), for which there is no conventional explanation in terms of environmental influences. The data of this experiment also contain further important characteristics which are important from the geophysical the point of view and for radon investigations in particular. The herein described further systematics of the temporal variation of nuclear radiation from radon in the experiment are summarized as follows:
1. A multi-year variation has probably been detected
2. Periodic signals occur in the annual, solar rotation (SR; around 30 days) and daily frequency bands
3. SR periodicity is evident in the gamma radiation from Bi-214
4. Annual periodicity dominates the long term variation
5. Semi-annual and ternary-annual variations occur. These multiples of the annual periodicity are physical phenomena
6. 24-hour periodicity is the primary daily variation

7. Multiples in the daily frequency band, of 12- and 8-hours (and possibly shorter) are observed in the time and frequency domains. They are considered to reflect physical effects, which at this stage are unexplained
8. A secondary influence occurs around 16 hours (UT)
9. Nonlinear coupling of the nuclear radiation occurs among the annual, SR and daily periodicities.
10. Directionality is observed in the gamma radiation from radon

Several features jointly (in combination) suggest, that more than one non-terrestrial driver may be involved:
1. Directionality – apparent in the difference of the HID patterns observed in up-down versus horizontal dimensions of the gamma radiation from radon in the tank.
2. Day-night difference in the maximum intensity (amplitude) of the annual and semi-annual periodicity.
3. Day-night difference in amplitude of Solar Rotation.

An alternative possibility might be that the day-night differences reflect, in part, modulation of a solar influence by bulk earth.

Large data sets of radon (alpha, gamma), measured at <1-hour resolution, have also been examined at geological locations. These investigations span a wide range of geologic settings in Israel and also abroad and reach a depth of hundreds of meters. Comparable basic statistical characteristics in the time, frequency and frequency-time domains are observed. The temporal variation consists of periodic signals in the annual and daily frequency bands and of non-periodic signals at a multi-day scale. Typically non-linear combinations among signal types are apparent. In-depth comparison of the characteristics of the periodic signals of radon time series and those in local atmospheric parameters - mainly P, T (above and subsurface) – have repeatedly demonstrated that it is unlikely that periodic signals observed in the radon data are being driven entirely by variations in environmental parameters, such as temperature and pressure. An important and enlightening case of geological radon is the alpha and gamma pattern of radon observed in the Gran Sasso (LNGS, Italy) facility, at stable temperature and depth of 1 km (Steinitz et al., 2013b). On the other hand the recurrent occurrence of daily and annual periodicities, and multiples thereof, led to raising the notion that a direct influence of a component in solar radiation drives the periodic signals of radon at depth [Steinitz et al., 2007, 2010a, 2010b,2013b, 2015].

So far ECM based radon investigations revealed phenomena and characteristics that correspond to those observed in geological radon. A series of experiments in the lab demonstrated that an external influence drives the variations in the nuclear radiation from radon inside the tight ECM canister. The latter are not due to mass transfer between the canister volume and the environment. The outcomes contributed to the notion of an above surface non-terrestrial influence. The indicators for such a notion are: a) radon variation in ECM experiments consist of periodic, and non-periodic signals of types similar to those encountered in geological radon; b) the statistical characteristics of the variation of the signal types and their combinations are comparable to those encountered in geological radon, and again c) the variation, albeit a general similarity, could not be attributed to local P and T variation. Furthermore, the ECM investigations added additional features of the nuclear radiation from radon in air: d) directionality and spatial inhomogeneity (3D) of the radiation of the radiation field; e) directionality in the variation seems to be related to global orientation – i.e. influenced by the rotation of Earth around its axis.

The notion of non-terrestrial influence on periodic components in radon was substantiated by identification of a solar rotational (SR) periodicity (~30 days, rotation of sun around its axis). Using a 3.5 year long data set, Sturrock et al. (2012) first showed this in the gamma radiation from radon in a multi-year reference ECM time series acquired at the GSI. Using an 8-year time series of gamma radiation in the same experiment allowed Sturrock et al. (2018) to refine and confirm the outcome, and present further evidence for non-terrestrial influence by demonstrating the influence of rotation of earth around its axis on the annual, semiannual and SR periodicities. The herein presented independent analysis as presented in Figures 14-16 underscores this conclusion.

As already implied in our previous works, claiming that variation in nuclear radiation from radon is reflecting an external influence is in apparent conflict with the prevailing view on the constancy of nuclear decay rates. Still, in the case of radon phenomena the evidence appears to show that decay rates are not all constant all of the time. Thus the accumulated geophysical and ECM derived evidence suggests a fundamental knowledge gap that has to be addressed by nuclear physicists.

Moreover, further investigations of the phenomena in the geo-sphere might help focus the issue for the nuclear physicists. The accumulated information and specifically this experiment allow formulation of new geophysical implications:

1. The non-terrestrial influence, whatever its exact nature is, influences radon at surface conditions, and in the subsurface to at least 1 km.
2. Earth bound local and regional geologic properties modify the non-terrestrial influence
3. Detection of the phenomena is improved by using high radon levels, i.e. increasing the number of radon atoms influencing the detector
4. Using ECM type systems allows the obtaining of significant resolution, and elimination of atmospheric type influences.

Data accessibility

The datasets supporting this article are available via file: ESM-C measured data.

Competing interests

We have no competing interests.

Authors contributions

GS ran the experiment, performed the data analysis and laid out the manuscript. OP performed the data collection, rectification, preprocessing and parts of the data analysis. PS contributed to the data

analysis and the evaluation of the results. EF participated in the evaluation of the results and in the design of the manuscript. All authors gave final approval for publication.

REFERENCES

Ball, T.K., Cameron, D.G., Colma, T.B. and Roberts, P.D., 1991. Behavior of radon in the geological environment: a review. Q. J. Eng. Geol., 24, 169-182.

Barbosa, S.M., Donner R.V., Steinitz, G. (Eds) 2015. Radon applications in geosciences – Progress & perspectives. Eur. Phys. J. Special Topics 224, 597–603 (2015) DOI: 10.1140/epjst/e2015-02393-y

Groves-Kirby, C. J., Denman, A. R., Crockett, R. G., Phillips, P. S., Gillmore, G. K., 2006. Identification of tidal and climatic influences within domestic radon time series from Northamptonshire, UK. Science of the Total Environ. 367, 191-202.

Hartmann, J. and Levy, J. K., 2005. Hydrogeological and gas geochemical earthquake precursors - A review for application. Nat. Hazards, 34, 279-304.

Monin, M.M., Seidel, J.L., 1992. Radon in soil-air and groundwater related to major geophysical events: a survey. Nuclear Instruments and Methods in Physics Research. Section A: Accelerators, Spectrometers, Detectors and Associated Equipment. 314 (2), 316-330.

Steinitz, G., Piatibratova, O., and Barbosa, S.M., 2007. Radon daily signals in the Elat Granite, southern Arava, Israel. J. Geophys. Res., 112, B10211, doi:10.1029/2006JB004817.

Steinitz, G. and Piatibratova, O., 2008. Experimental replication of radon signals that occur in the geological environment. Israel. Geol. Surv. Rep. GSI/17/08, 45p.

Steinitz, G., Piatibratova, O., 2010a. Radon signals in the Gavnunim intrusion, Makhtesh Ramon, Israel. Geophys. J. Int. 180, 651–665.

Steinitz, G. and Piatibratova, O., 2010b. Radon signals at the Roded site, Southern Israel. Solid Earth, 1, 99-109, doi:10.5194/se-1-99-2010.

Steinitz, G., Piatibratova, O. & Kotlarsky, P., 2011. Possible effect of solar tides on radon signals. *Journal of Environmental Radioactivity 102, 749-765, doi:http://dx.doi.org/10.1016/j.jenvrad.2011.04.002*.

Steinitz, G., Kotlarsky, P., Piatibratova, O., 2013a. Anomalous non-isotropic temporal variation of gamma-radiation from radon (progeny) within air in confined conditions. Geophysical Journal International, 193, 1110-1118; doi: 10.1093/gji/ggt057

Steinitz, G., Piatibratova, O. and Charit-Yaari, N., 2013b. Influence of a component of solar irradiance on radon signals at 1 km depth, Gran Sasso, Italy. *Proc. R. Soc. A,* 469 2159, 20130411; doi:10.1098/rspa.2013.0411.

Steinitz, G., Piatibratova, O., and Kotlarsky, P., 2014. Sub-daily periodic radon signals in a confined radon system. Journal of Environmental Radioactivity 134C (2014), 128-135.

Steinitz, G., Martin-Luis, M.C., Piatibratova, O., 2015. Indications for solar influence on radon signal in the subsurface of Tenerife (Canary Islands, Spain). European Physical Journal – Special Topics. Eur. Phys. J. Special Topics, 224, 687–695 (2015). DOI: 10.1140/epjst/e2015-02399-5

Steinitz G., Kotlarsky P., Piatibratova O., 2016. Indications for influence of artificial (man-made) activity on radon signals, in simulation experiments. *Proc. R. Soc. A* **472** 20160311. http://dx.doi.org/10.1098/rspa.2016.0311

Sturrock, P. A., Steinitz, G., Fischbach, E., Javorsek Ii, D. & Jenkins, J. H., 2012. Analysis of gamma radiation from a radon source: Indications of a solar influence. *Astroparticle Physics* **36**, 18-25, doi:http://dx.doi.org/10.1016/j.astropartphys.2012.04.009.

Sturrock, P.A., Steinitz, G., Fischbach, E., 2018. Analysis of gamma radiation from a radon source. II, Indications of influences of both solar and cosmic neutrinos on beta decays. Astroparticle Physics [In press].

Toutain, J.P., Baubron, J.C., 1999. Gas geochemistry and seismotectonics: a review. Tectonophysics 304, 1-27.

Zafrir, H., Haquin, G., Malik, U., Barbosa, S.M., Piatibratova, O., Steinitz, G., 2011. Gamma versus Alpha Sensors for Rn-222 Long-Term Monitoring in Geological Environments. Radiation Measurements, 46, 611-620. doi:10.1016/j.radmeas.2011.04.027.

Figures

Indications for non-terrestrial influences on radon signals from a multi-year enhanced confined experiment
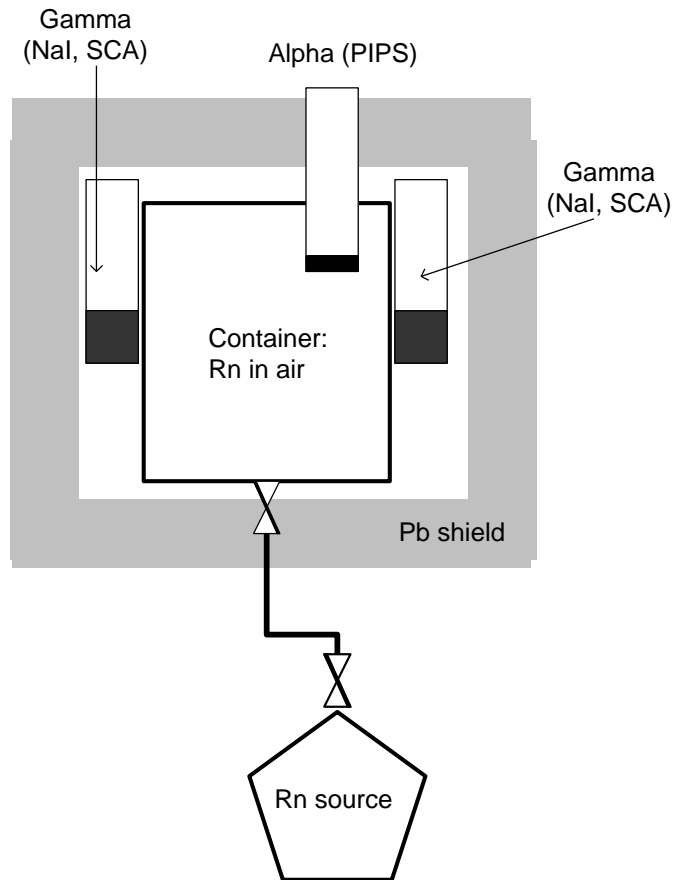
ESM - Figures
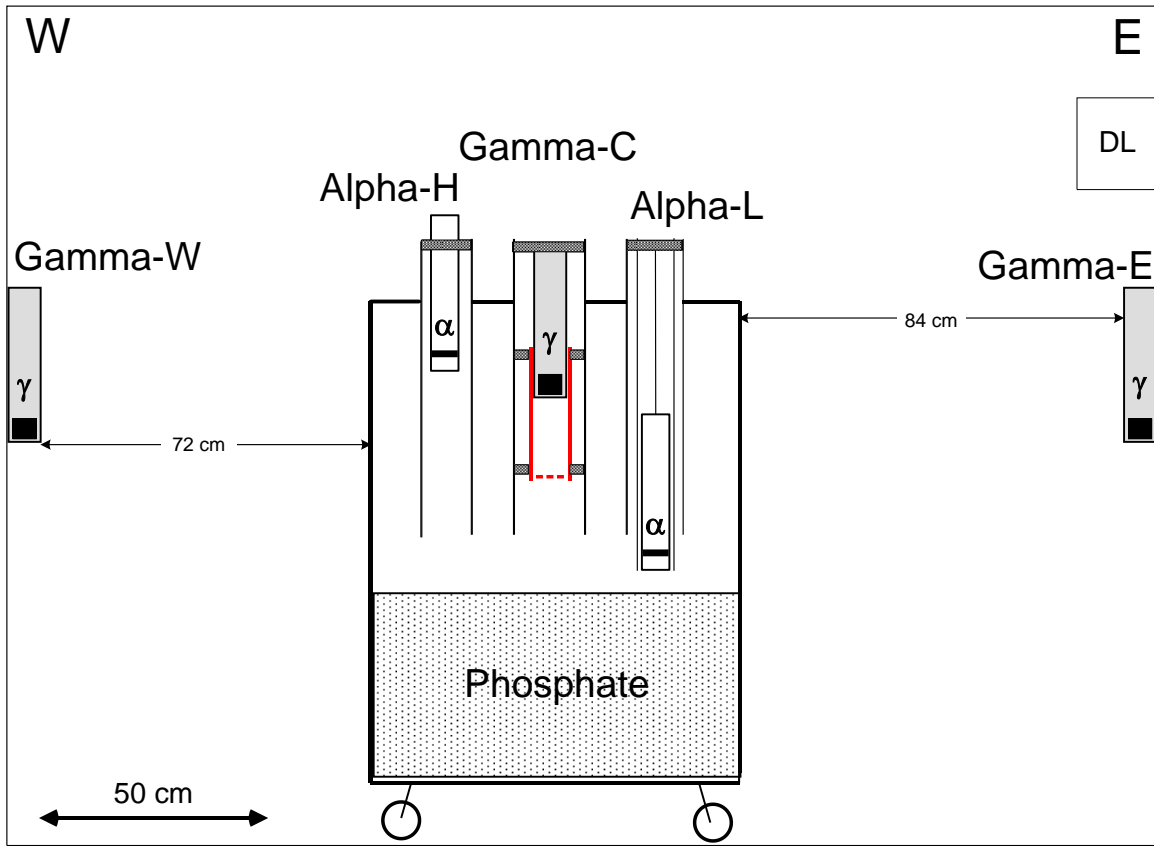
Figure 1: The ECM principle

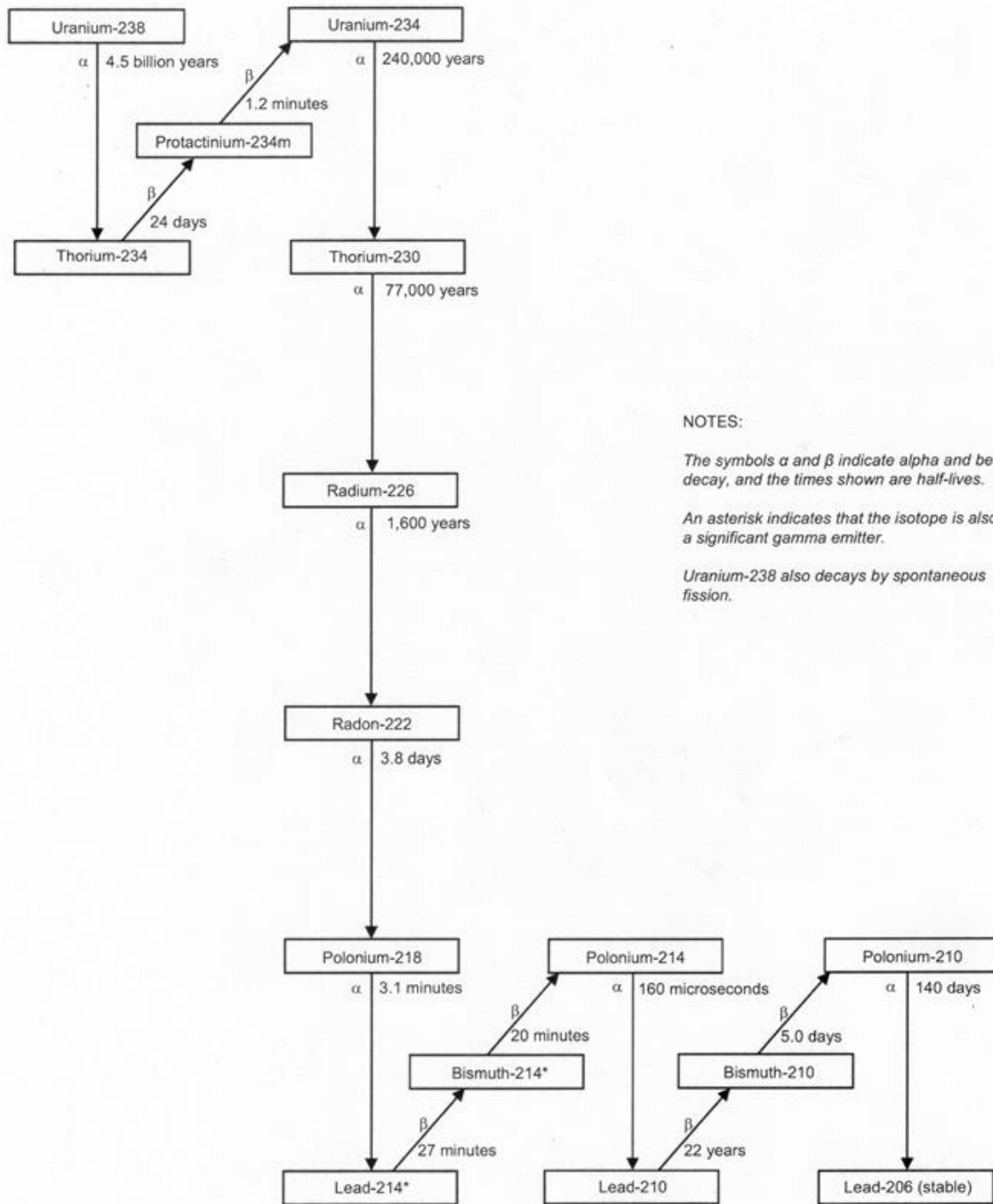Figure 2: Layout of EXP #1. Gamma-C is inserted inside a 0.5 cm thick pipe (red).

Figure 3: Decay chain of Uranium-238. (Courtesy of Argonne National Laboratory).
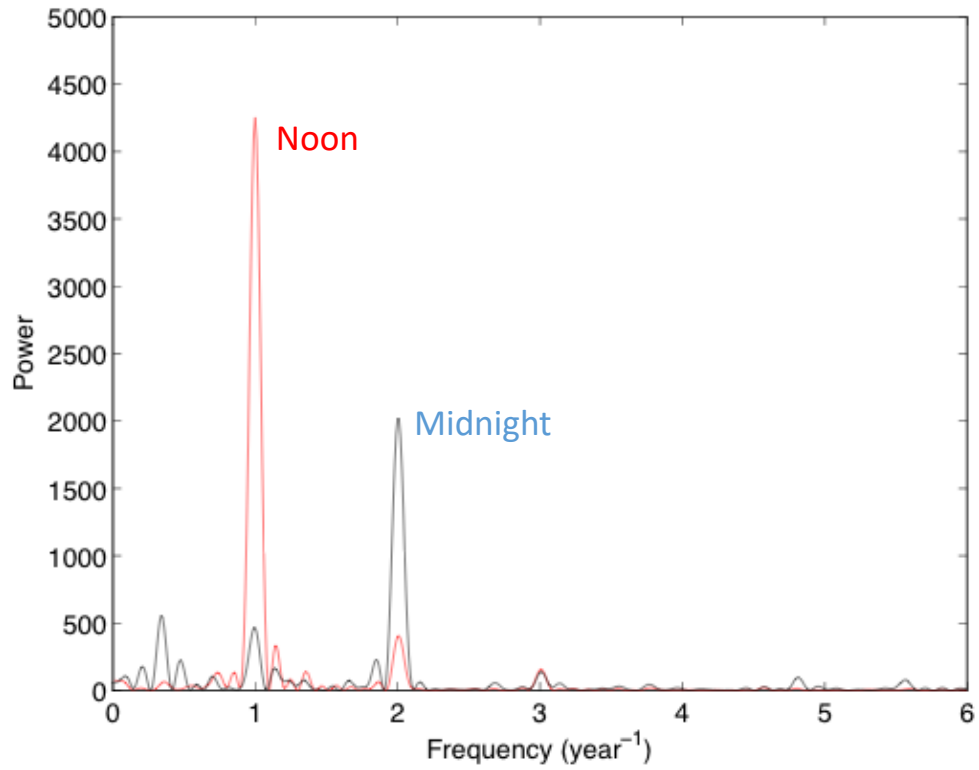
Figure 4: Power spectrum of g-C centered on noon (red) and midnight (blue) in the frequency band of 0-6 year-1. Reproduced from Sturrock et al., 2018.
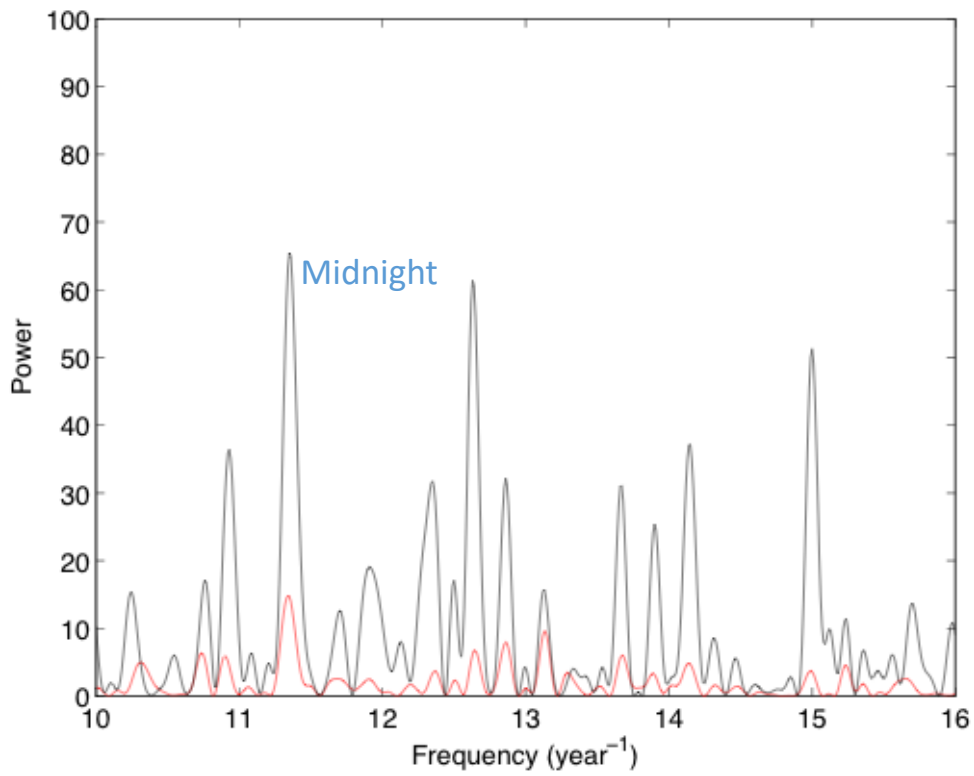

Figure 5: Power spectrum of g-C centered on noon (red) and midnight (blue) in the frequency band of 10-16 year-1. Reproduced from Sturrock et al., 2018.

Eventual influence of local environmental variations

The eventual influence of local conditions – instrumental effects and atmospheric - on the radon signal in EXP #1 was extensively elaborated and discussed by Steinitz et al. (2011), in the framework of an environmentally oriented publication platform. Due its importance an excerpt and summary is given below.

Radon alpha and gamma measurement techniques applied are described in detail by Zafrir et al (2011). Further specific details are given by Steinitz and Piatibratova (2008). The specifications of the instruments indicate linearity in the span of ambient temperature. The detector systems (and data logger) are industrial products and frequently utilized, since the 1990"s, in geological and environmental radon surveys. Investigations performed since 1995 by the GSI at diverse field locations and in the laboratory utilize the same industrial systems types (models), while demonstrating their robustness.

The setup of EXP #1 is enclosed within a tight 640 liter tank. It is located above ground under an open shack. The source of radon is a ground phosphorite rock originating from an open pit mine in southern Israel, containing around 120 ppm of Uranium. The ground material is emanating radon into its pores, from where it is supplied by diffusion to the overlying air volume, in which the gamma and alpha sensors are immersed. Primary situational and environmental factors are [Steinitz et al., 2011]:

- The tank wall, made of iron plates, is in thermal equilibrium with the surrounding ambient temperature.
- Internal pressure is in equilibrium with the atmospheric pressure.
- Local conditions led to large temperature variations, from daily to annual scale, spanning some 40°C.
- Slow mixing in the upper volume of air is assumed due to convection inside the tank.
- The tank is in part of the day under direct influence of sunlight.
- The internal radon sensors are in complete darkness.

Investigations of variation patterns of ^{222}Rn in the geological environment applied the common practice of comparison with atmospheric parameters in the time domain or in frequency domain. Such analysis leads to ambiguities and inconclusiveness in terms of interpretation. For a review see Barbosa et al. (2015). Applying advanced analysis of the phenomena in the combined frequency-time domain (MTWF, Steinitz et al, 2007) demonstrated for the first time systematics of radon characteristics that differ extensively from those in temperature and pressure. This formed the basis for claiming that apparent similarity (in the time domain) of signal patterns of radon versus temperature and/or pressure does not substantiate causality. Applying such analysis to several radon time series originating from very different geological situations confirmed the same situation [Steinitz and Piatibratova 2010a,b; Steinitz et al. 2013a; Steinitz et al. 2015]. In a further step, the specific systematics of the periodic signals in the daily and annual frequency bands, combined with the lack of tidal gravity periodicity, led to the suggestion that a component in solar radiation is driving these signals directly.

A similar analysis approach in the frequency-time domain was applied to evaluate the time series of EXP #1 (Steinitz et al., 2011). Due to its above surface location it is influenced by large environmental variation, and therefore considered as under very unfavorable conditions. The Moving-Time-Window Fourier spectral analysis [Steinitz and Piatibratova 2007; Steinitz et al. 2011]. was applied to examine the characteristics of variation in the combined frequency-time domain. The amplitudes of the daily periodic components of the atmospheric pressure, ambient temperature and measured radon signal were derived from FFT spectra calculated per consecutive time intervals. In the case of radon (gamma,. alpha) ratios of the normalized diurnal (24-hour) versus sub-diurnal (12-hour) amplitudes align along a linear pattern, while dispersed patterns are derived for the atmospheric parameters (Figure 21 in Steinitz et al. 2011). It was argued that the dispersed patterns of the atmospheric parameters cannot generate the regular linear pattern observed for the alpha and gamma radiation signal from ^{222}Rn and its progeny. This test was performed on the measured data using a simple statistical analysis, and its outcome is independent of other considerations and modes of analysis. As such the test is robust, and the outcome is therefore considered as an indicative criterion. The results from such examinations of data from EXP #1 do not support the notion of a direct connection between the temporal variation of the ^{222}Rn signal and atmospheric influences, and probably negate it.

Further considerations as to an eventual influence of temperature and/or pressure are arrived at from the analysis presented in the previous sections, and are discussed below.